Adaptive projective synchronization of different chaotic systems with nonlinearity inputs*

Niu Yu-Jun(牛玉军)[a)†], Wang Xing-Yuan(王兴元)[b)], and Pei Bing-Nan(裴炳南)[a)]

[a)] *School of Information Engineering, Dalian University, Dalian* 116622, *China*

[b)] *School of Electronic & Information Engineering, Dalian University of Technology, Dalian* 116024, *China*

(Received 3 August 2011; revised manuscript received 25 September 2011)

We investigate the projective synchronization of different chaotic systems with nonlinearity inputs. Based on the adaptive technique, sliding mode control method and pole assignment technique, a novel adaptive projective synchronization scheme is proposed to ensure the drive system and the response system with nonlinearity inputs can be rapidly synchronized up to the given scaling factor.

Keywords: projective synchronization, adaptive technique, sliding mode control, nonlinearity input

PACS: 05.45.Gg, 05.45.Xt, 05.45.Vx **DOI:** 10.1088/1674-1056/21/3/030503

1. Introduction

In 1990, Pecora and Carroll presented the concept of "chaotic synchronization" for the first time[1] and introduced a method to synchronize two identical chaotic systems with different initial conditions.[2] Nowadays chaotic synchronization has been intensively studied.[3−9] Different types of chaotic synchronization methods have been achieved, such as complete synchronization, generalized synchronization, phase synchronization, and lag synchronization.[10−15] In coupled partially linear systems, Mainieri and Rehacek reported that the two identical systems (drive and response) could be synchronized up to a scaling factor. This type of chaotic synchronization is referred to as projective synchronization.[16] In applications to secure communications, projective synchronization can be used to extend binary digital to M-nary digital communication for achieving fast communication, so projective synchronization has raised great concern and been further studied.[17−29] For example, Xu and Li[17,18] have presented the stability criterion of projective synchronization of three-dimensional chaotic systems, the judge criterion of projective synchronization of any dimensional continuous chaotic systems and the necessary condition of projective synchronization of any dimensional discrete chaotic system; the projective synchronization technique has been applied to chaotic secure communications.[19−21] Recently, by Lyapunov stability theory, the adaptive control law and the parameter update law have been derived to make the states of two different chaotic systems asymptotically synchronized up to a desired scaling function.[22] Zhang and Lu[28] also extended the concept of projective synchronization to the one of full state hybrid projective synchronization in two different chaotic systems. Hung *et al.*[29] have designed the adaptive sliding mode controller to achieve the projective synchronization of Chua's systems with a dead-zone in the control input. However, in the studies mentioned above and many other existing projective synchronization studies, the projective synchronization of different chaotic systems and nonlinearity input are not considered simultaneously.

In practical situations, in systems such as laser array, biological systems and cognitive processes, it is hardly the case that every component can be assumed to be identical. In addition, in recent years, more and more applications of chaos synchronization in secure communications make it much more important to achieve the projective synchronization of the two different chaotic systems. In addition, in practical applications, owing to physical limitations, there always exist nonlinear effects in the control actuators.[30] Neglecting the effect of input nonlinearities usually results in degeneration of system performance.

*Project supported by the National Natural Science Foundation of China (Grant Nos. 60971107 and 60973152) and the Natural Science Foundation of Liaoning Province, China (Grant No. 20082165).

†Corresponding author. E-mail: yujun_niu@163.com

© 2012 Chinese Physical Society and IOP Publishing Ltd

Variable structure controllers with a sliding mode were proposed by Utkin,[31] and have been widely recognized as a powerful approach to control problems. The main advantage of this approach is that the variable structure can be potentially exploited to improve control performance such as robustness and fast time response. The variable structure control strategy is based on the concept of an attractive manifold, upon which the underlying state of vector space and the desired dynamic is assured. During the sliding motion, the system has invariance properties and is independent of parameter uncertainty and disturbance.

Therefore, in this paper, we study the projective synchronization of different chaotic systems, in the presence of parameter uncertainty, noise disturbance and nonlinearity inputs. A proportional-integral switching surface is designed to guarantee the stability of the projective synchronization error dynamics system in sliding mode, and an adaptation law is given to estimate the bound values of system uncertainties and noise disturbance. Consequently, by applying the adaptation law, a robust adaptive sliding mode controller can be constructed to ensure the occurrence of a sliding motion. The different chaotic systems with nonlinearity inputs can be rapidly synchronized up to the given scaling factor, even without knowing the boundary of parameter uncertainties and noise disturbance. Finally, numerical simulations for uncertain unified chaotic systems are performed to demonstrate the effectiveness and feasibility of the proposed scheme.

2. System description and problem formulation

We consider two different chaotic systems described by

$$\dot{\boldsymbol{x}} = \boldsymbol{A}\boldsymbol{x} + \boldsymbol{h}(\boldsymbol{x}), \tag{1}$$

and

$$\dot{\boldsymbol{y}} = \boldsymbol{B}\boldsymbol{y} + \boldsymbol{g}(\boldsymbol{y}) + \Delta\boldsymbol{f}(\boldsymbol{y}) + \boldsymbol{d}(t) + \boldsymbol{\Phi}(\boldsymbol{u}), \tag{2}$$

where $\boldsymbol{x} \in R^n$ is an n-dimensional state vector of system (1), the $\boldsymbol{A} \in R^{n\times n}$ is the coefficient matrix of the linear part of system (1), $\boldsymbol{h}(\boldsymbol{x}) : R^n \to R^n$ is a nonlinear smooth function and is the nonlinear part of system (1). Correspondingly, $\boldsymbol{y}$, $\boldsymbol{B}$ and $\boldsymbol{g}(\boldsymbol{y})$ are n-dimensional state vector, the coefficient matrix of the linear part and nonlinear part of system (2), respectively. The $\Delta\boldsymbol{f}(\boldsymbol{y})$ and $\boldsymbol{d}(t)$ are the parameter uncertainty and noise disturbance applied to system (2), respectively. The $\boldsymbol{\Phi}(\boldsymbol{u}) = [\phi_1(u_1), \phi_2(u_2), \ldots, \phi_n(u_n)]^{\mathrm{T}}$, $\phi_i(u_i)$ $(i = 1, 2, \ldots, n)$ is a nonlinear function, $\phi_i(u_i) = 0$ for $-u_{i0-} \le u_i \le u_{i0+}$, and $\phi_i(u_i)$ is assumed to satisfy the following inequalities:

$$\begin{cases} \alpha_{i1}(u_i - u_{i0+})^2 \le (u_i - u_{i0+})\phi_i(u_i) \le \alpha_{i2}(u_i - u_{i0+})^2, & (u_i > u_{i0+}), \\ \alpha_{i1}(u_i + u_{i0-})^2 \le (u_i + u_{i0-})\phi_i(u_i) \le \alpha_{i2}(u_i + u_{i0-})^2, & (u_i < -u_{i0-}), \end{cases} \tag{3}$$

where α_{i1} and α_{i2} are nonzero positive constants. For the i-th input u_i, the nonlinear input function $\phi_i(u_i)$ is shown in Fig. 1.

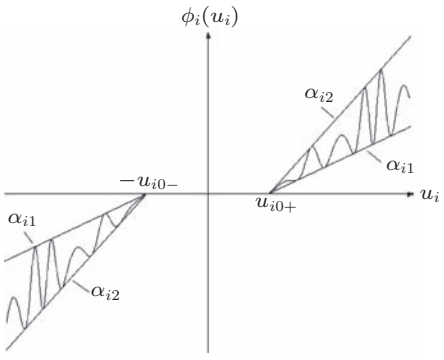


Fig. 1. Nonlinear function $\phi_i(u_i)$ for the i-th input u_i.

System (1) and system (2) are defined as the drive and response systems, respectively. The projective synchronization error between system (1) and system (2) is defined as $\boldsymbol{e} = \boldsymbol{y} - \lambda\boldsymbol{x}$, so the error dynamics system is determined by the following equation:

$$\begin{aligned} \dot{\boldsymbol{e}} = \dot{\boldsymbol{y}} - \lambda\dot{\boldsymbol{x}} = {} & (\boldsymbol{B} - \boldsymbol{A})\boldsymbol{y} + \boldsymbol{A}\boldsymbol{e} + \boldsymbol{g}(\boldsymbol{y}) - \lambda\boldsymbol{h}(\boldsymbol{x}) \\ & + \Delta\boldsymbol{f}(\boldsymbol{y}) + \boldsymbol{d}(t) + \boldsymbol{\Phi}(\boldsymbol{u}), \end{aligned} \tag{4}$$

where λ is a nonzero constant, and is a scaling factor defining a proportional relation between the synchronized systems. Hence, complete synchronizations and anti-synchronizations are the special cases of projective synchronization when the scaling factor $\lambda = 1$ and $\lambda = -1$, respectively.

The aim of this study, without the requirement

of bounds of uncertainties and disturbances, is to design an adaptive sliding mode controller for holding the following formula:

$$\lim_{t\to\infty}\|\boldsymbol{e}\| = \lim_{t\to\infty}\|\boldsymbol{y} - \lambda\boldsymbol{x}\| = 0. \tag{5}$$

Thus, system (1) and system (2) can be synchronized up to the given scaling factor even with parameter uncertainties, external noise disturbance and nonlinearity inputs.

3. Design of the switching surface and adaptive sliding mode controller

Achieving projective synchronization of system (1) and system (2) involves two major steps. The first step is to select an appropriate switching surface which can guarantee the asymptotic stability of the projective synchronization error dynamics system in the sliding mode. The second step is to determine an adaptive sliding mode controller which can guarantee the occurrence of sliding motion, can be strongly robust to nonlinearity inputs, and can estimate the bounds of parameter uncertainties and noise disturbance. To achieve this aim, a proportional-integral switching function is suggested to be

$$\boldsymbol{S}(t) = \boldsymbol{e}(t) - \int_0^t (\boldsymbol{A} - \boldsymbol{K})\boldsymbol{e}(\tau)\,\mathrm{d}\tau, \tag{6}$$

where $\boldsymbol{S}(t) = [s_1(t), s_2(t), \ldots, s_n(t)]^{\mathrm{T}}$ is a switching surface vector. The $\boldsymbol{K} \in R^{n\times n}$ is a constant matrix and $\boldsymbol{K}$ is chosen such that the real part of the eigenvalues of $(\boldsymbol{A} - \boldsymbol{K})$ are all negative.

It is well known that when the system operates in the sliding mode, the following equations must be satisfied:[31,32]

$$\boldsymbol{S}(t) = \boldsymbol{e}(t) - \int_0^t (\boldsymbol{A} - \boldsymbol{K})\boldsymbol{e}(\tau)\,\mathrm{d}\tau = 0, \tag{7}$$

and

$$\dot{\boldsymbol{S}} = \dot{\boldsymbol{e}} - (\boldsymbol{A} - \boldsymbol{K})\boldsymbol{e} = 0. \tag{8}$$

From Eq. (8), we have

$$\dot{\boldsymbol{e}} = (\boldsymbol{A} - \boldsymbol{K})\boldsymbol{e}. \tag{9}$$

From Eq. (9), it reveals that when the pair $(\boldsymbol{A}, \boldsymbol{I})$ is controllable, using a pole assignment technique, we find that there exists a constant gain matrix $\boldsymbol{K}$ such that the real part of the eigenvalues of $(\boldsymbol{A} - \boldsymbol{K})$ are all negative. Therefore, according to the stability criterion of a linear system, Equation (5) is satisfied. Furthermore, the convergence rate of Eq. (9) can be determined by $\boldsymbol{K}$.

To ensure the occurrence of sliding motion, a sliding mode controller is designed as

$$u_i(t) = \begin{cases} -\gamma_i\eta_i\,\mathrm{sign}(s_i(t)) - u_{i0-}, & (s_i(t) > 0), \\ 0, & s_i(t) = 0, \\ -\gamma_i\eta_i\,\mathrm{sign}(s_i(t)) + u_{i0+}, & s_i(t) < 0, \end{cases} \tag{10}$$

where $\eta_i = |(b_i - a_i)\boldsymbol{y} + g_i(\boldsymbol{y}) - \lambda h_i(\boldsymbol{x})| + |k_i\boldsymbol{e}| + \hat{\theta}_i$, $(i = 1, 2, \ldots, n)$; a_i and b_i are the i-th row vector of matrices $\boldsymbol{A}$ and $\boldsymbol{B}$, respectively; $\gamma_i = \beta/\alpha_{i1}$, β is a positive constant and larger than 1, α_{i1} is the same as that of Eq. (3); $s_i(t)$ $(i = 1, 2, \ldots, n)$ is the component of the switching surface vector $\boldsymbol{S}(t) = [s_1(t), s_2(t), \ldots, s_n(t)]^{\mathrm{T}}$; $\mathrm{sign}(s_i(t))$ is the sign function of $s_i(t)$, (if $s_i(t) > 0$, $\mathrm{sign}(s_i(t)) = 1$; if $s_i(t) = 0$, $\mathrm{sign}(s_i(t)) = 0$; if $s_i(t) < 0$, $\mathrm{sign}(s_i(t)) = -1$); $\hat{\theta}_i$ is an estimate parameter which satisfies the following adaptive law:

$$\dot{\hat{\theta}}_i = |S_i|\,, \quad \hat{\theta}_i(0) = \hat{\theta}_{i0}, \tag{11}$$

where $\hat{\theta}_{i0}$ is the positive and bounded initial value of $\hat{\theta}_i$. Let $|\Delta f_i(\boldsymbol{y}) + d_i(t)|$ be bounded, that is, $|\Delta f_i(\boldsymbol{y}) + d_i(t)| < \theta_i$, but θ_i is an unknown positive constant value. Now define the adaptation error of $\hat{\theta}_i$ as

$$\tilde{\theta}_i = \hat{\theta}_i - \theta_i. \tag{12}$$

Since θ_i is an existing constant, it yields

$$\dot{\tilde{\theta}}_i = \dot{\hat{\theta}}_i = |S_i|\,. \tag{13}$$

In what follows, the proposed adaptive sliding mode controller (10) will be proved to be able to ensure the existence of sliding motion and achieve the projective synchronization of system (1) and system (2).

Theorem 1 Consider the drive system (1) and response system (2) controlled by the sliding mode controller (10). Then the trajectory of the projective synchronization error dynamics Eq. (4) converges to the sliding surface $\boldsymbol{S} = 0$.

Proof Consider the following Lyapunov function candidate as

$$V = 0.5(\boldsymbol{S}^{\mathrm{T}}(t)\boldsymbol{S}(t) + \tilde{\boldsymbol{\theta}}^{\mathrm{T}}\tilde{\boldsymbol{\theta}}).$$

Using differentiation and substituting Eqs. (4) and (8) into the time derivative of V, we obtain

$$
\begin{aligned}
\dot{V} &= \boldsymbol{S}^{\mathrm{T}}(t)\dot{\boldsymbol{S}}(t) + \tilde{\boldsymbol{\theta}}^{\mathrm{T}}\dot{\tilde{\boldsymbol{\theta}}} \\
&= \boldsymbol{S}^{\mathrm{T}}(t)(\dot{\boldsymbol{e}} - (\boldsymbol{A}-\boldsymbol{K})\boldsymbol{e}) + \tilde{\boldsymbol{\theta}}^{\mathrm{T}}\dot{\tilde{\boldsymbol{\theta}}} \\
&= \boldsymbol{S}^{\mathrm{T}}(t)((\boldsymbol{B}-\boldsymbol{A})\boldsymbol{y} + \boldsymbol{A}\boldsymbol{e} + \boldsymbol{g}(\boldsymbol{y}) - \lambda\boldsymbol{h}(\boldsymbol{x}) + \Delta\boldsymbol{f}(\boldsymbol{y}) + \boldsymbol{d}(t) + \boldsymbol{\Phi}(\boldsymbol{u}) - (\boldsymbol{A}-\boldsymbol{K})\boldsymbol{e}) + \tilde{\boldsymbol{\theta}}^{\mathrm{T}}\dot{\tilde{\boldsymbol{\theta}}} \\
&= \boldsymbol{S}^{\mathrm{T}}(t)((\boldsymbol{B}-\boldsymbol{A})\boldsymbol{y} + \boldsymbol{g}(\boldsymbol{y}) - \lambda\boldsymbol{h}(\boldsymbol{x}) + \boldsymbol{K}\boldsymbol{e} + \Delta\boldsymbol{f}(\boldsymbol{y}) + \boldsymbol{d}(t)) + \boldsymbol{S}^{\mathrm{T}}(t)\boldsymbol{\Phi}(\boldsymbol{u}) + \tilde{\boldsymbol{\theta}}^{\mathrm{T}}\dot{\tilde{\boldsymbol{\theta}}} \\
&= \sum_{i=1}^{n}[s_i(t)((b_i-a_i)\boldsymbol{y} + g_i(\boldsymbol{y}) - \lambda h_i(\boldsymbol{x}) + k_i\boldsymbol{e} + \Delta f_i(\boldsymbol{y}) + d_i(t)) + s_i(t)\phi_i(u_i)_i + \tilde{\theta}_i\dot{\tilde{\theta}}_i] \\
&\leq \sum_{i=1}^{n}[|s_i(t)|\,(|(b_i-a_i)\boldsymbol{y} + g_i(\boldsymbol{y}) - \lambda h_i(\boldsymbol{x})| + |k_i\boldsymbol{e}| + \theta_i) + \tilde{\theta}_i\dot{\tilde{\theta}}_i + s_i(t)\phi_i(u_i)] \\
&= \sum_{i=1}^{n}[|s_i(t)|\,(|(b_i-a_i)\boldsymbol{y} + g_i(\boldsymbol{y}) - \lambda h_i(\boldsymbol{x})| + |k_i\boldsymbol{e}| + \hat{\theta}_i - \tilde{\theta}_i) + \tilde{\theta}_i|s_i(t)| + s_i(t)\phi_i(u_i)] \\
&= \sum_{i=1}^{n}[|s_i(t)|\,(|(b_i-a_i)\boldsymbol{y} + g_i(\boldsymbol{y}) - \lambda h_i(\boldsymbol{x})| + |k_i\boldsymbol{e}| + \hat{\theta}_i) + s_i(t)\phi_i(u_i)] \\
&= \sum_{i=1}^{n}[|s_i(t)|\,\eta_i + s_i(t)\phi_i(u_i)]. \qquad (14)
\end{aligned}
$$

When $s_i > 0$, we obtain

$$
\begin{aligned}
(u_i + u_{i0-})\varphi_i(u_i) &= -\gamma_i\eta_i\,\mathrm{sign}(s_i(t))\varphi_i(u_i) \\
&\geq \alpha_{i1}(u_i + u_{i0-})^2 \\
&= \alpha_{i1}\gamma_i^2\eta_i^2[\mathrm{sign}(s_i(t))]^2. \qquad (15)
\end{aligned}
$$

when $s_i < 0$, we have

$$
\begin{aligned}
(u_i - u_{i0+})\varphi_i(u_i) &= -\gamma_i\eta_i\,\mathrm{sign}(s_i(t))\varphi_i(u_i) \\
&\geq \alpha_{i1}(u_i - u_{i0+})^2 \\
&= \alpha_{i1}\gamma_i^2\eta_i^2[\mathrm{sign}(s_i(t))]^2. \qquad (16)
\end{aligned}
$$

Since $s_i^2(t) \geq 0$, from Eqs. (15) and (16), we have

$$
\begin{aligned}
&-\gamma_i\eta_i s_i(t)^2\,\mathrm{sign}(s_i(t))\phi_i(u_i) \\
&\geq \alpha_{i1}\gamma_i^2\eta_i^2 s_i(t)^2[\mathrm{sign}(s_i(t))]^2.
\end{aligned}
$$

Therefore, we obtain

$$
\begin{cases}
-\gamma_i\eta_i s_i(t)\phi_i(u_i) \geq \alpha_{i1}\gamma_i^2\eta_i^2\,|s_i(t)|\,, \\
s_i(t)\phi_i(u_i) \leq -\alpha_{i1}\gamma_i\eta_i\,|s_i(t)|\,.
\end{cases} \qquad (17)
$$

By replacing inequality (17) with (14), we obtain

$$
\begin{aligned}
\dot{V} &= \boldsymbol{S}^{\mathrm{T}}(t)\dot{\boldsymbol{S}}(t) + \tilde{\boldsymbol{\theta}}^{\mathrm{T}}\dot{\tilde{\boldsymbol{\theta}}} \\
&\leq \sum_{i=1}^{n}(1-\alpha_{i1}\gamma_i)\eta_i\,|s_i(t)| \leq 0. \qquad (18)
\end{aligned}
$$

Let $w(t) = \sum_{i=1}^{n}(\alpha_{i1}\gamma_i - 1)\eta_i\,|s_i(t)|$, we have

$$
\dot{V} \leq -w(t) \leq 0. \qquad (19)
$$

Integrating the above equation from zero to t, we have

$$
V(0) \geq V(t) + \int_0^t w(\nu)\,\mathrm{d}\nu \geq \int_0^t w(\nu)\,\mathrm{d}\nu. \qquad (20)
$$

As t goes to infinity, the above integral is always less than or equal to $V(0)$. Since $V(0)$ is positive and finite, $\lim_{t\to\infty}\int_0^t w(\nu)\,\mathrm{d}\nu$ exists and is finite. Thus, according to Barbalat lemma,[33] we obtain

$$
\lim_{t\to\infty} w(t) = \lim_{t\to\infty}\sum_{i=1}^{n}(\alpha_{i1}\gamma_i - 1)\eta_i\,|s_i(t)| = 0. \qquad (21)
$$

Since $(\alpha_{i1}\gamma_i - 1)\eta_i > 0$, we have $\lim_{t\to\infty}\sum_{i=1}^{n}|s_i(t)| = \lim_{t\to\infty} s(t) = 0$. Hence, the proof is completely achieved.

4. Numerical simulation

Using the above adaptive sliding mode controller, we investigate the projective synchronization of the two pairs of different chaotic systems (Lorenz–Chen and Chen–Lü) with nonlinearity inputs. The Lorenz system[34] is described by the following nonlinear equations:

$$
\begin{cases}
\dot{x}_1 = -\rho_1 x_1 + \rho_1 x_2, \\
\dot{x}_2 = \rho_2 x_1 - x_2 - x_1 x_3, \\
\dot{x}_3 = x_1 x_2 - \rho_3 x_3.
\end{cases} \qquad (22)
$$

When $\rho_1 = 10$, $\rho_2 = 28$ and $\rho_3 = 8/3$, this system has a chaotic attractor as shown in Fig. 2(a). Chen system[35] is a typical chaos anti-control model, and it can be described by

$$
\begin{cases}
\dot{y}_1 = -\nu_1 y_1 + \nu_1 y_2, \\
\dot{y}_2 = (\nu_2 - \nu_1)y_1 - y_1 y_3 + \nu_2 y_2, \\
\dot{y}_3 = y_1 y_2 - \nu_3 y_3.
\end{cases} \qquad (23)
$$

The Chen system indicates the chaotic attractor as shown in Fig. 2(b) when $\nu_1 = 35$, $\nu_2 = 28$, and $\nu_3 = 3$. The third chaotic system is Lü system,[36] which connects the Lorenz and Chen attractors and is represented by

$$\begin{cases} \dot{z}_1 = -\omega_1 z_1 + \omega_1 z_2, \\ \dot{z}_2 = -z_1 z_3 + \omega_2 z_2, \\ \dot{z}_3 = z_1 z_2 - \omega_3 z_3. \end{cases} \tag{24}$$

The Lü system has a chaotic attractor as shown in Fig. 2(c), when $\omega_1 = 36$, $\omega_2 = 20$, and $\omega_3 = 3$. In what follows, we will apply the present control law to achieve the projective synchronization for two pairs of the given chaotic systems.

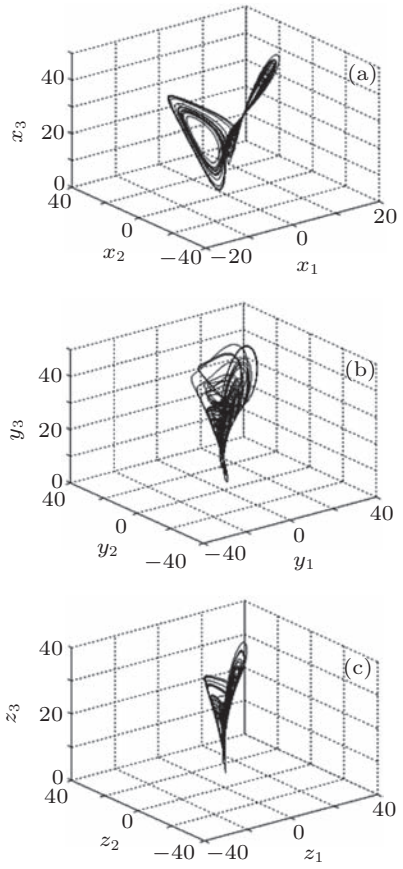


Fig. 2. Chaos system attractors: (a) Lorenz attractor, (b) Chen attractor, (c) Lü attractor.

4.1. Projective synchronization between Lorenz and Chen systems

Chen system with nonlinearity inputs is written as

$$\begin{cases} \dot{y}_1 = -\nu_1 y_1 + \nu_1 y_2 + \Delta f_1(y) + d_1(t) + \phi_1, \\ \dot{y}_2 = (\nu_2 - \nu_1) y_1 - y_1 y_3 + \nu_2 y_2 \\ \qquad +\Delta f_2(y) + d_2(t) + \phi_2, \\ \dot{y}_3 = y_1 y_2 - \nu_3 y_3 + \Delta f_3(y) + d_3(t) + \phi_3. \end{cases} \tag{25}$$

System (22) and system (25) are defined as the drive and response systems, respectively. Obviously the matrices $\boldsymbol{A}$, $\boldsymbol{B}$, $\boldsymbol{h}(\boldsymbol{x})$ and $\boldsymbol{g}(\boldsymbol{y})$, respectively, are

$$\boldsymbol{A} = \begin{bmatrix} -\rho_1 & \rho_1 & 0 \\ \rho_2 & -1 & 0 \\ 0 & 0 & -\rho_3 \end{bmatrix}, \quad \boldsymbol{B} = \begin{bmatrix} -\nu_1 & \nu_1 & 0 \\ \nu_2 - \nu_1 & \nu_2 & 0 \\ 0 & 0 & -\nu_3 \end{bmatrix},$$
$$\boldsymbol{h}(\boldsymbol{x}) = \begin{bmatrix} 0 \\ -x_1 x_3 \\ x_1 x_2 \end{bmatrix}, \quad \boldsymbol{g}(\boldsymbol{y}) = \begin{bmatrix} 0 \\ -y_1 y_3 \\ y_1 y_2 \end{bmatrix}. \tag{26}$$

Since the matrix $\left[\boldsymbol{I},\ \boldsymbol{A} \times \boldsymbol{I},\ \boldsymbol{A}^2 \times \boldsymbol{I}\right]$ is in full rank, $(\boldsymbol{A}, \boldsymbol{I})$ is controllable. Therefore, we can construct the gain vector $\boldsymbol{K}$ by the pole placement technique. To ensure the convergence of system (4), that is to say that Eq. (5) is satisfied, we select the eigenvalues of $(\boldsymbol{A} - \boldsymbol{K})$ as $\left[-1,\ -2,\ -3\right]$. So the gain vector $\boldsymbol{K}$ is computed as

$$\boldsymbol{K} = \begin{bmatrix} -9 & 10 & 0 \\ 28 & 1 & 0 \\ 0 & 0 & 1/3 \end{bmatrix}. \tag{27}$$

Furthermore, it is supposed that the uncertainty term

$$\Delta \boldsymbol{f} = [\Delta f_1,\ \Delta f_2,\ \Delta f_3]^{\mathrm{T}} = [0.1 y_1,\ 0.1 y_2,\ 0.1 y_3]^{\mathrm{T}}$$

and external disturbance

$$\begin{aligned} \boldsymbol{d}(t) &= [d_1(t),\ d_2(t),\ d_3(t)]^{\mathrm{T}} \\ &= [0.2\cos(2\pi t),\ 0.3\cos(3\pi t),\ 0.4\cos(4\pi t)]^{\mathrm{T}} \end{aligned}$$

in these two projective synchronization examples. Nonlinear function $\phi_i(u_i)$ of $u_i (i = 1, 2, 3)$ is defined as

$$\phi_1(u_1) = \begin{cases} [0.8 + 0.1\sin(u_1)](u_1 - u_{10+}), & (u_1 > u_{10+}), \\ 0, & (-u_{10-} \le u_1 \le u_{10+}), \\ [0.8 + 0.1\sin(u_1)(u_1 + u_{10-}), & (u_1 < -u_{10-}), \end{cases} \tag{28}$$

$$\phi_2(u_2) = \begin{cases} [0.8 + 0.2\sin(u_2)](u_2 - u_{20+}), & (u_2 > u_{20+}), \\ 0, & (-u_{20-} \le u_2 \le u_{20+}), \\ [0.8 + 0.2\sin(u_2)](u_2 + u_{20-}), & (u_2 < -u_{20-}), \end{cases} \tag{29}$$

$$\phi_3(u_3) = \begin{cases} 0.9 + 0.3\sin(u_3)](u_3 - u_{30+}), & (u_3 > u_{30+}), \\ 0, & (-u_{30-} \le u_3 \le u_{30+}), \\ [0.9 + 0.3\sin(u_3)](u_3 + u_{30-}), & (u_3 < -u_{30-}). \end{cases} \tag{30}$$

From Eqs. (28)–(30), we obtain $\alpha_{11} = 0.7$, $\alpha_{21} = 0.6$, $\alpha_{31} = 0.6$. $\hat{\theta}_{10} = \hat{\theta}_{20} = \hat{\theta}_{30} = 1$ and $\beta = 1.01$ are chosen. It is assumed that $u_{10-} = u_{10+} = 1$, $u_{20-} = u_{20+} = 2$, $u_{30-} = u_{30+} = 3$. The above parameters meet the requirement of Theorem 1.

The initial values of the drive system (22) and response system (25) are $(x_1(0),\ x_2(0),\ x_3(0)) = (1, 2, 3)$ and $(y_1(0),\ y_2(0),\ y_3(0)) = (5, 8, 12)$, respectively. The scaling factor λ is respectively selected as 2, -2 and -0.5. Simulation results of projective synchronization are shown in Figs. 3–6. From Fig. 3, we can see that the errors $e_1(t)$, $e_2(t)$ and $e_3(t)$ have been rapidly stabilized to zero. Namely, system (25) has synchronized with system (22). Figures 4–6 show that state variable amplitudes of system (25) are respectively 2 times, 2 times and 0.5 times those of system (22), whereas the phases of system (25) and system (22) are in-phase, anti-phase and anti-phase, respectively, namely the attractors of system (25) and system (22) synchronize up to the given scaling factor.

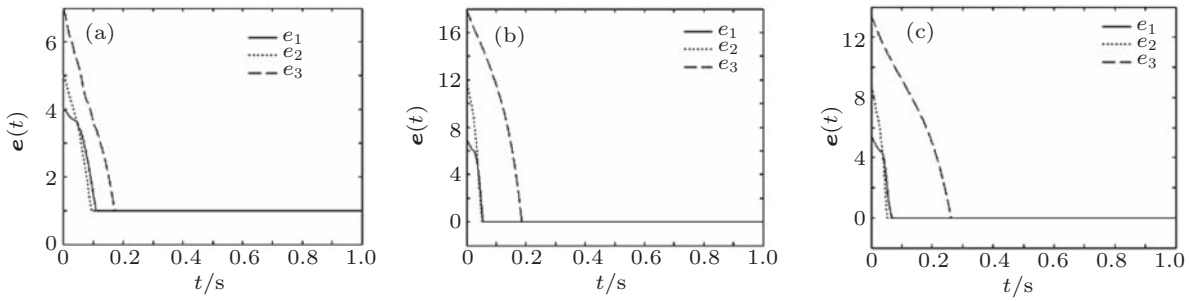


Fig. 3. The projective synchronization errors between system (22) and system (25): (a) $\lambda = 2$, (b) $\lambda = -2$, (c) $\lambda = -0.5$.

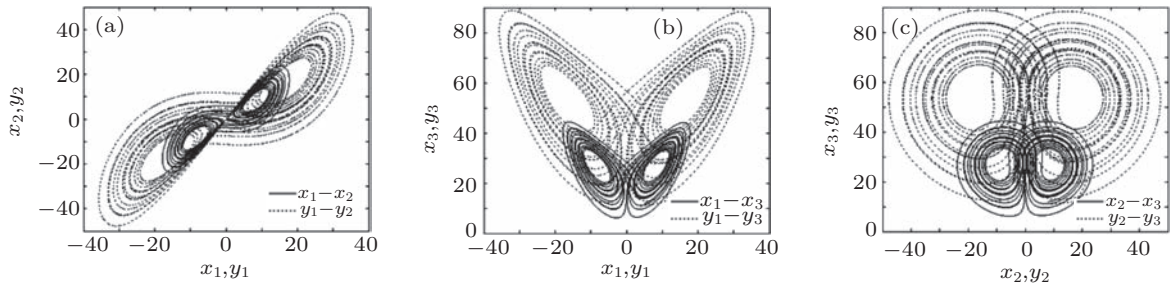


Fig. 4. The projection of attractors of system (22) and system (25) on the two-dimensional plane, when $\lambda = 2$. (a) x_1–x_2, y_1–y_2; (b) x_1–x_3, y_1–y_3; (c) x_2–x_3, y_2–y_3.

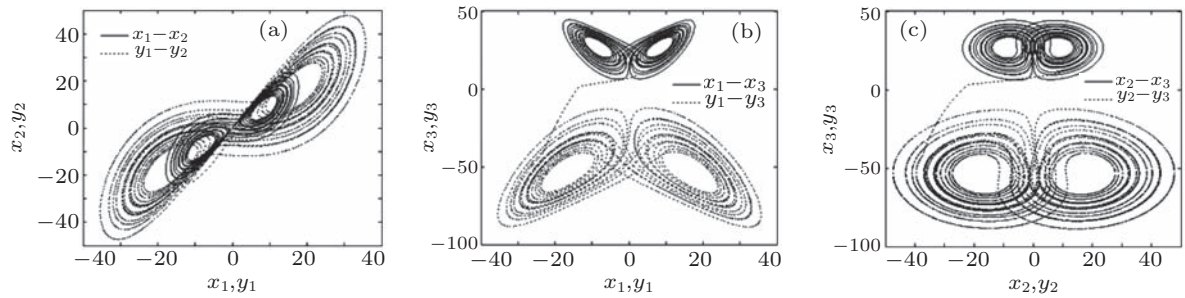


Fig. 5. The projection of attractors of system (22) and system (25) on the two-dimensional plane, when $\lambda = -2$. (a) x_1–x_2, y_1–y_2; (b) x_1–x_3, y_1–y_3; (c) x_2–x_3, y_2–y_3.

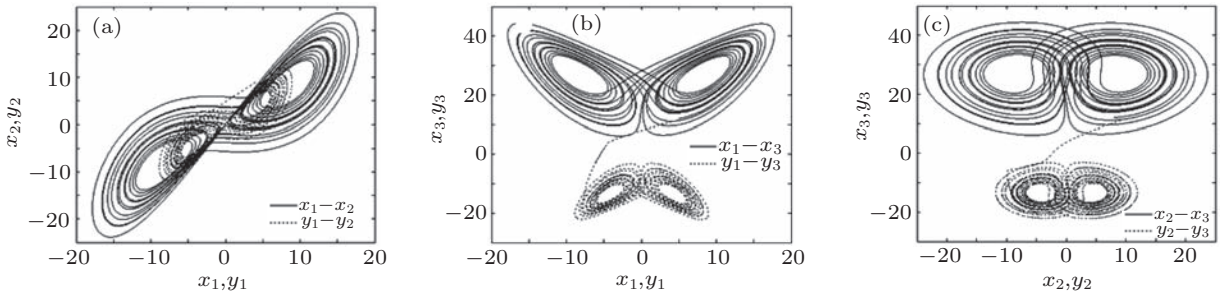


Fig. 6. The projection of attractors of system (22) and system (25) on the two-dimensional plane, when $\lambda = -0.5$. (a) x_1–x_2, y_1–y_2; (b) x_1–x_3, y_1–y_3; (c) x_2–x_3, y_2–y_3.

4.2. Projective synchronization between Chen and Lü systems

Lü system with nonlinearity inputs is described by

$$\begin{cases} \dot{z}_1 = -\omega_1 z_1 + \omega_1 z_2 + \Delta f_1(z) + d_1(t) + \phi_1, \\ \dot{z}_2 = -z_1 z_3 + \omega_2 z_2 + \Delta f_2(z) + d_2(t) + \phi_2, \\ \dot{z}_3 = z_1 z_2 - \omega_3 z_3 + \Delta f_3(z) + d_3(t) + \phi_3. \end{cases} \quad (31)$$

System (23) and system (31) are defined as the drive and response systems, respectively. Therefore, the matrices $\boldsymbol{A}$, $\boldsymbol{B}$, $\boldsymbol{h}(\boldsymbol{y})$ and $\boldsymbol{g}(\boldsymbol{z})$, respectively, are

$$\boldsymbol{A} = \begin{bmatrix} -\nu_1 & \nu_1 & 0 \\ \nu_2 - \nu_1 & \nu_2 & 0 \\ 0 & 0 & -\nu_3 \end{bmatrix},$$

$$\boldsymbol{B} = \begin{bmatrix} -\omega_1 & \omega_1 & 0 \\ 0 & \omega_2 & 0 \\ 0 & 0 & -\omega_3 \end{bmatrix},$$

$$\boldsymbol{h}(\boldsymbol{y}) = \begin{bmatrix} 0 \\ -y_1 y_3 \\ y_1 y_2 \end{bmatrix}, \quad \boldsymbol{g}(\boldsymbol{z}) = \begin{bmatrix} 0 \\ -z_1 z_3 \\ z_1 z_2 \end{bmatrix}. \quad (32)$$

The matrix $[\,\boldsymbol{I},\ \boldsymbol{A}\times\boldsymbol{I},\ \boldsymbol{A}^2\times\boldsymbol{I}\,]$ is in full rank, therefore, we select the eigenvalues of $(\boldsymbol{A}-\boldsymbol{K})$ as $[\,-1,\ -2,\ -1\,]$. Using the pole placement technique, the gain vector $\boldsymbol{K}$ is computed to be

$$\boldsymbol{K} = \begin{bmatrix} -34 & 35 & 0 \\ -7 & 30 & 0 \\ 0 & 0 & -2 \end{bmatrix}. \quad (33)$$

Values of nonlinear function $\phi_i(u_i)(i = 1, 2, 3)$ are the same as the ones of 4.1. We choose $\hat{\theta}_{10} = \hat{\theta}_{20} = \hat{\theta}_{30} = 2$ and $\beta = 1.01$. The above parameters meet the requirement of Theorem 1.

The initial values of the drive system (23) and response system (31) are $(y_1(0),\ y_2(0),\ y_3(0)) = (5, 8, 12)$ and $(z_1(0),\ z_2(0),\ z_3(0)) = (2, 4, 8)$, respectively. The scaling factor λ is respectively selected as 2, -1 and -0.5. Simulation results of projective synchronization are shown in Figs. 7–10, which show that system (31) and system (23) synchronize up to the given scaling factor.

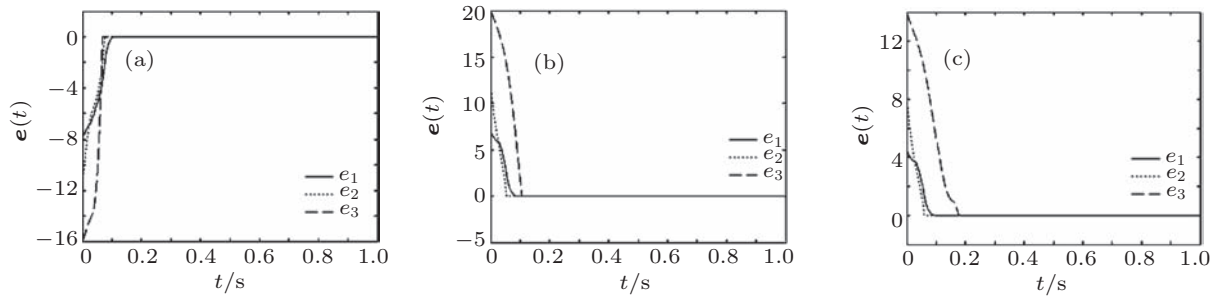


Fig. 7. The projective synchronization errors between system (23) and system (31): (a) $\lambda = 2$, (b) $\lambda = -1$, (c) $\lambda = -0.5$.

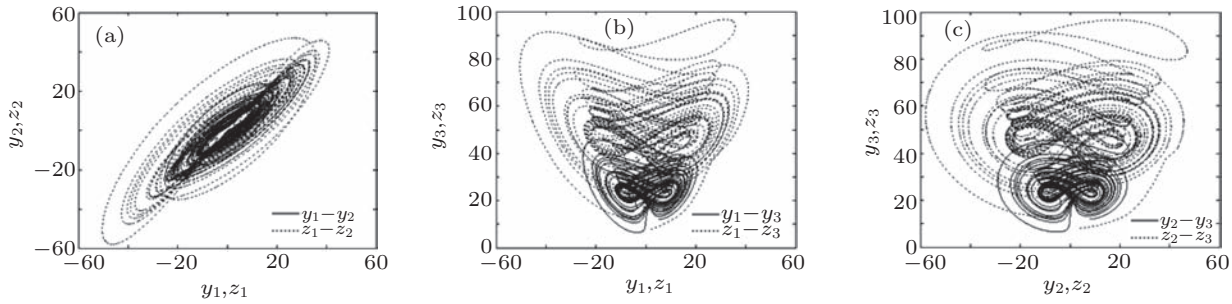


Fig. 8. The projection of attractors of system (23) and system (31) on the two-dimensional plane when $\lambda = 2$. (a) y_1–y_2, z_1–z_2; (b) y_1–y_3, z_1–z_3; (c) y_2–y_3, z_2–z_3.

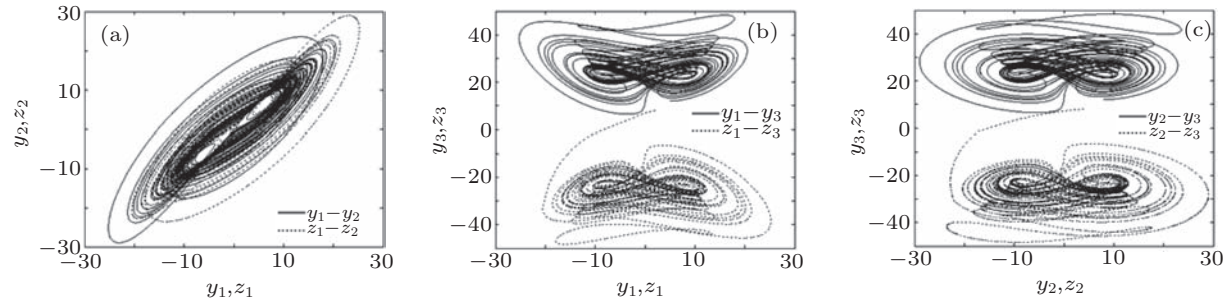


Fig. 9. The projection of attractors of system (23) and system (31) on the two-dimensional plane when $\lambda = -1$. (a) y_1–y_2, z_1–z_2; (b) y_1–y_3, z_1–z_3; (c) y_2–y_3, z_2–z_3.

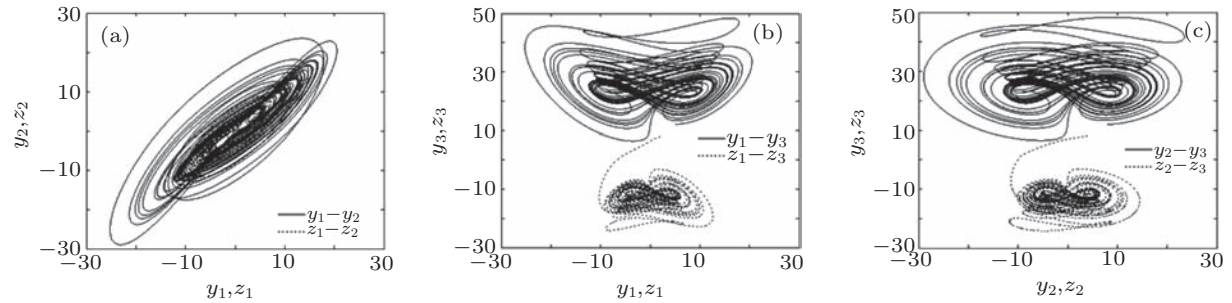


Fig. 10. The projection of attractors of system (23) and system (31) on the two-dimensional plane when $\lambda = -0.5$. (a) y_1–y_2, z_1–z_2; (b) y_1–y_3, z_1–z_3; (c) y_2–y_3, z_2–z_3.

5. Conclusion

In this paper, a novel adaptive projective synchronization scheme of different chaotic systems is proposed to ensure that the drive system and the response system can be rapidly synchronized up to the given scaling factor. The results of numerical simulation for the two pairs of different chaotic systems (Lorenz–Chen and Chen–Lü) further verify the effectiveness and feasibility of the proposed scheme.

A comparison with the aforementioned method shows the advantages of the proposed approach as follows: 1) the proposed scheme can overcome the controller with input nonlinearity; 2) the design controller is robust to the parameter uncertainties and noise disturbance, without requiring the bounds of the parameter uncertainties and noise disturbance; 3) the proposed method can be further extended to the projective synchronization of different chaotic systems with more state variables.

References

[1] Pecora L M and Carroll T L 1990 *Phys. Rev. Lett.* **64** 821
[2] Carroll T L and Pecora L M 1991 *IEEE Trans. Circuits Syst.* **38** 453
[3] Chen G and Dong X 1993 *IEEE Trans. Circuits Syst.* I **40** 591

[4] An H L and Chen Y 2008 *Chin. Phys.* B **17** 98
[5] Chen G and Dong X 1998 *From Chaos to Order: Methodologies, Perspectives and Applications* (Singapore: World Scientific)
[6] Yang D S, Zhang H G, Zhao Y, Song C H and Wang Y C 2010 *Acta Phys. Sin.* **59** 1562 (in Chinese)
[7] Zhang H, Xie Y, Wang Z and Zheng C 2007 *IEEE Trans. Neural Networks* **18** 1841
[8] Zhang R X and Yang S P 2008 *Chin. Phys.* B **17** 4097
[9] Zou Y L and Zhu J 2006 *Chin. Phys.* **15** 1965
[10] Shinbrot T, Grebogi C, Yorke J and Ott E 1993 Nature **363** 411
[11] Jia Z, Lu J A, Deng G M and Zhang Q J 2007 *Chin. Phys.* **16** 1246
[12] Zhang H G, Ma T D, Fu J and Tong S C 2009 *Chin. Phys.* B **18** 3742
[13] Wang X Y and Zhao Q 2008 *Acta Phys. Sin.* **57** 2812 (in Chinese)
[14] Li C L and Luo X S 2009 *Acta Phys. Sin.* **58** 3759 (in Chinese)
[15] Liu Z B, Zhang H G and Sun Q Y 2010 *Chin. Phys.* B **19** 090506
[16] Mainieri R and Rehacek J 1999 *Phys. Rev. Lett.* **82** 3042
[17] Xu D and Li Z 2002 *Int. J. Bifurcation and Chaos* **12** 1395
[18] Li Z and Xu D 2001 *Phys. Lett.* A **282** 175
[19] Chee C Y and Xu D 2005 *Chaos Solitons Fract.* **23** 1063
[20] Li K Z, Zhao M C and Fu X C 2009 *IEEE Trans Circuits Syst.* I **56** 2280
[21] Hu M F and Xu Z Y 2007 *Chin. Phys.* **16** 3231
[22] Du H Y, Zeng Q S and Wang C H 2008 *Phys. Lett.* A **372** 5402
[23] Dai H, Jia L X, Hui M and Si G Q 2011 *Chin. Phys.* B **20** 040507
[24] Lü L, Chai Y and Luan L 2010 *Chin. Phys.* B **19** 080506
[25] Wang X Y and He Y J 2008 *Acta Phys. Sin.* **57** 1485 (in Chinese)
[26] Luo L X, Xu Z Y and Hu M F 2008 *Chin. Phys.* B **17** 4067
[27] Zeng C Y, Sun M and Tian L X 2010 *Acta Phys. Sin.* **59** 5288 (in Chinese)
[28] Zhang Q J and Lu J A 2007 *Phys. Lett.* A **372** 1416
[29] Hung Y C, Yan J J and Liao T L 2008 *Math. Comput. Simulat.* **77** 374
[30] Gutierrez H M and Ro P I 1998 *IEEE Trans. Ind. Electron.* **45** 921
[31] Utkin V I 1978 *Sliding Mode and Their Application in Variable Structure Systems* (Moscow: Mir)
[32] Itkis U 1976 *Control System of Variable Structure* (New York: Wiley)
[33] Popov V M 1973 *Hyperstability of Control System* (Berlin: Springer-Verlag)
[34] Lorenz E N 1963 *J. Atmos Sci.* **20** 130
[35] Chen G and Ueta T 1999 *Int. J. Bifurcation and Chaos* **9** 1465
[36] Lü J and Chen G 2002 *Int. J. Bifurcation and Chaos* **12** 659